

Article

The Boundary Integral Equation for Kinetically Limited Dendrite Growth

Ekaterina A. Titova ¹, Peter K. Galenko ², Margarita A. Nikishina ¹, Liubov V. Toropova ³
and Dmitri V. Alexandrov ^{1,*}

¹ Laboratory of Multi-Scale Mathematical Modeling, Department of Theoretical and Mathematical Physics, Ural Federal University, Lenin Ave., 51, Ekaterinburg 620000, Russia; ekatitova@mail.ru (E.A.T.); margarita.nikishina@urfu.ru (M.A.N.)

² Otto-Schott-Institut für Materialforschung, Friedrich-Schiller-Universität-Jena, 07743 Jena, Germany; peter.galenko@uni-jena.de

³ Laboratory of Mathematical Modeling of Physical and Chemical Processes in Multiphase Media, Department of Theoretical and Mathematical Physics, Ural Federal University, Lenin Ave., 51, Ekaterinburg 620000, Russia; l.v.toropova@urfu.ru

* Correspondence: dmitri.alexandrov@urfu.ru

Abstract: The boundary integral equation defining the interface function for a curved solid/liquid phase transition boundary is analytically solved in steady-state growth conditions. This solution describes dendrite tips evolving in undercooled melts with a constant crystallization velocity, which is the sum of the steady-state and translational velocities. The dendrite tips in the form of a parabola, paraboloid, and elliptic paraboloid are considered. Taking this solution into account, we obtain the modified boundary integral equation describing the evolution of the patterns and dendrites in undercooled binary melts. Our analysis shows that dendritic tips always evolve in a steady-state manner when considering a kinetically controlled crystallization scenario. The steady-state growth velocity as a factor that is dependent on the melt undercooling, solute concentration, atomic kinetics, and other system parameters is derived. This expression can be used for determining the selection constant of the stable dendrite growth mode in the case of kinetically controlled crystallization.

Keywords: boundary integral equation; moving boundary problem; phase transition; curved solid–liquid interface; undercooled liquid; dendrite

MSC: 82B26



Citation: Titova, E.A.; Galenko, P.K.; Nikishina, M.A.; Toropova, L.V.; Alexandrov, D.V. The Boundary Integral Equation for Kinetically Limited Dendrite Growth. *Axioms* **2023**, *12*, 1016. <https://doi.org/10.3390/axioms12111016>

Academic Editor: Zacharias A. Anastassi

Received: 22 September 2023

Revised: 20 October 2023

Accepted: 27 October 2023

Published: 28 October 2023



Copyright: © 2023 by the authors. Licensee MDPI, Basel, Switzerland. This article is an open access article distributed under the terms and conditions of the Creative Commons Attribution (CC BY) license (<https://creativecommons.org/licenses/by/4.0/>).

1. Introduction

Phase transformations from nonequilibrium and metastable states to the solid form are widespread in nature (the freezing of water, the solidification of magma, etc.) and are often used in technological processes and laboratory facilities to obtain alloys with certain structures and properties, as well as for the synthesis of various compounds in the chemical and pharmacological industries. This explains extensive studies of directional and bulk crystallization in the phase transformation region consisting of simultaneous liquid and solid phases [1–6]. As this takes place, the evolution of the solid/liquid phase interface in an undercooled or supersaturated liquid is responsible for the processes of impurity redistribution between the growing solid phase elements, pattern development, and microstructure formation. Therefore, the problem of the mathematical description of a phase transformation can be reduced to the problem of the evolution of a solid/liquid phase interface.

A single integral differential equation defining its evolution in an undercooled one-component liquid was derived for the first time by Nash and Glicksman [7,8]. This equation for the interface function was then extended for binary systems solidifying in

local-equilibrium and local-nonequilibrium conditions [9,10], as well as for convective thermodiffusion problems [11–13]. An important point is that the boundary integral equation (BIE) represents the basis for the morphological stability analysis of dendritic crystals and the selection of their stable growth modes [14–22]. Moreover, the BIE is a formal solution of various Stefan-like problems and can be used for the numerical modeling of pattern formation and evolution [23]. In addition, the BIE can also be used for the verification of crystal growth theories and the comparison of model conclusions with computations carried out, for example, by the phase-field and enthalpy-based methods or by using direct simulations of moving-boundary problems [24–28].

It is well known that dendritic crystals reach steady-state growth very quickly [29–33]. Moreover, the solid–liquid interface may reach the kinetic regime of growth when approaching the steady state. Only the attachment/detachment of particles (atoms and molecules) at the interface controls the intensity of the interface migration. Special interest in the analysis of the kinetic mode of growth is also seen in the following:

- the explanations of the sharp transition from thermally controlled to kinetically limited regimes of growth [34–37];
- the interpretation of the data of molecular dynamics where the interface is governed by interfacial undercooling, i.e., by “kinetic undercooling” [38–41].

Taking a special interest in the study of stationary kinetic modes into account, we analyze the BIE for a unidirectional stationary crystallization scenario with a steady-state velocity V_{ss} and show that the crystal tip evolves with a constant velocity $V = V_{ss} + V_{tr}$ in the same reference frame (here, V_{tr} is a constant translational velocity in the moving reference frame). The theory under question is formulated for two- and three-dimensional problems describing a stable growth mode of dendritic crystals whose tips represent a parabola, paraboloid and elliptic paraboloid.

2. Two-Dimensional BIE for Solidifying Pure Liquid

Let us first consider the simplest case of dendritic growth in a single-component undercooled liquid with a constant (steady-state) velocity V_{ss} in a laboratory reference frame (see Figure 1). We introduce a characteristic spatial scale ρ and time scale ρ/V_{ss} , where ρ can be the diameter of the crystal tip or the doubled radius of the curvature. Let us write down the two-dimensional BIE for the solidification of the pure (chemically one-component) liquid with the interface function $\zeta(x, t)$ by assuming these scales as follows [9] (see also the Appendix A):

$$\Delta - \frac{d_c}{\rho} K(x, t) - \beta V_{ss} - \beta V_{ss} \frac{\partial \zeta(x, t)}{\partial t} = I_{\zeta}^T(x, t), \quad I_{\zeta}^T(x, t) = \frac{P_T}{2\pi} \int_0^{\infty} \frac{d\tau}{\tau} \int_{-\infty}^{\infty} dx_1 \times \left(1 + \frac{\partial \zeta(x_1, t - \tau)}{\partial t} \right) \exp \left[-\frac{P_T}{2\tau} \left((x - x_1)^2 + (\zeta(x, t) - \zeta(x_1, t - \tau) + \tau)^2 \right) \right]. \tag{1}$$

Here, $\Delta = c_p(T_0 - T_{\infty})/Q$ is the dimensionless undercooling, c_p is the thermal capacity, Q is the latent crystallization heat, T_0 is the phase transition temperature, T_{∞} is the liquid temperature far from the solid/liquid interface ζ , K is the interface curvature, d_c is the capillary length, β is the kinetic coefficient, $P_T = \rho V_{ss}/(2D_T)$ is the Péclet number, D_T is the thermal diffusivity, and x and t are the dimensionless spatial and time variables, respectively. Equation (1) describes the interface motion, with velocity V_{ss} defining the driving force Δ , interface curvature $K \propto \rho^{-1}$, and the heat transport outgoing the interface; see the r.h.s. of Equation (1). Note that Δ , d_c , ρ , β , V_{ss} , and P_T in Equation (1) are assumed to be constant. The interface function $\zeta(x, t)$ should be found as a solution of this equation. Equation (1) must be supplemented with appropriate initial and boundary conditions. As an initial condition, one should choose a certain shape of the interface function $\zeta(x, t)$, e.g., a parabola, as is done below. It is also necessary to set boundary conditions reflecting the geometry of solidification region.

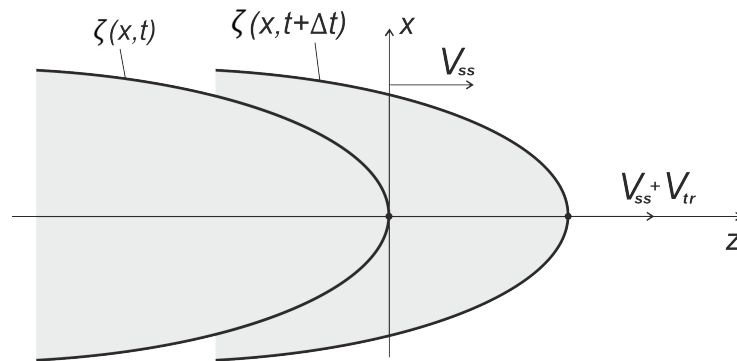


Figure 1. A scheme of a dendritic tip evolving in a steady-state manner along the spatial axis z .

In the present work, we consider the special case of negligible heat transport to govern the interface motion. This situation is well known in atomistic simulations where the interface motion in melting and crystallization is dictated by the atomistic kinetics at the interface, and the computational domain has (almost) uniform temperature [38–41]. In this case, the r.h.s. of the BIE (1) can be omitted. Additionally, we only consider the motion of the crystal tip, where the interface curvature is $K \approx -\partial^2\zeta/\partial x^2$.

Taking this into account, we rewrite Equation (1) as

$$(\Delta - \beta V_{ss}) \frac{\rho}{d_c} + \frac{\partial^2 \zeta}{\partial x^2} - \frac{\beta V_{ss} \rho}{d_c} \frac{\partial \zeta}{\partial t} = 0.$$

We solve this equation using the Laplace integral transform with respect to the time variable t . By introducing the Laplace variable p and Laplace image $\zeta^*(x, p) = \zeta^*(x)$ of the interface function $\zeta(x, t)$ as

$$\zeta^*(x) = \int_0^\infty \exp(-pt) \zeta(x, t) dt,$$

we obtain the following equation in the Laplace image space:

$$\frac{\Delta - \beta V_{ss}}{p} \frac{\rho}{d_c} + \frac{d^2 \zeta^*}{dx^2} - \frac{\beta V_{ss} p \rho}{d_c} \zeta^* + \frac{\beta V_{ss} \rho}{d_c} \zeta(x, 0) = 0. \tag{2}$$

Here, we have taken into account the following Laplace transform formula:

$$\zeta(x, t) \rightarrow p \zeta^*(x) - \zeta(x, 0), \quad \text{const.} \rightarrow \frac{\text{const.}}{p}.$$

The solution of Equation (2) reads as

$$\begin{aligned} \zeta^*(x) = & \frac{\sqrt{A}}{2\sqrt{p}} \exp(-\sqrt{pA}x) \int_0^\infty (\zeta(x_1, 0) - \zeta(-x_1, 0)) dx_1 + \frac{\Delta\rho - Ad_c}{p^2 Ad_c} \\ & + \frac{\sqrt{A}}{2} \left[\int_x^\infty \frac{\exp[-\sqrt{pA}(x_1 - x)]}{\sqrt{p}} \zeta(x_1, 0) dx_1 + \int_{-\infty}^x \frac{\exp[\sqrt{pA}(x_1 - x)]}{\sqrt{p}} \zeta(x_1, 0) dx_1 \right], \end{aligned} \tag{3}$$

where $A = \beta V_{ss} \rho / d_c$.

Let us assume $\zeta(x, 0) = -x^2/2$ as the initial condition for the interface function in the form of a parabola. By substituting $\zeta(x, 0)$ into (3), we arrive at

$$\zeta^*(x) = \frac{\Delta\rho - Ad_c}{p^2 Ad_c} - \frac{\sqrt{A}}{4\sqrt{p}} \left[\int_x^{+\infty} \exp(\sqrt{pA}(x - x_1)) x_1^2 dx_1 + \int_{-\infty}^x \exp(\sqrt{pA}(x_1 - x)) x_1^2 dx_1 \right]. \tag{4}$$

By integrating the r.h.s. of Equation (4), we obtain

$$\zeta^*(x) = \left(\frac{\Delta\rho - Ad_c}{Ad_c} - \frac{1}{A} \right) \frac{1}{p^2} - \frac{x^2}{2p}. \tag{5}$$

By calculating the inverse Laplace transform of Equation (5), we come to [42,43]

$$\zeta(x, t) = \left(\frac{\Delta\rho - Ad_c}{Ad_c} - \frac{1}{A} \right) t - \frac{x^2}{2}. \tag{6}$$

Expression (6) shows that the dendrite grows in a moving reference frame with the following constant translational velocity:

$$V_{tr} = V_{ss} \left(\frac{\Delta - \beta V_{ss}}{\beta V_{ss}} - \frac{d_c}{\beta V_{ss} \rho} \right). \tag{7}$$

This means that the dendrite evolves with the velocity $V = V_{ss} + V_{tr}$ in the laboratory reference frame. As is easily seen, the contribution of V_{tr} is caused by atomic kinetics (parameter β). Figure 2 shows the interface function $\zeta(x, t)$ versus the rescaled undercooling $\Delta/(\beta V)$ (panel (a)) and spatial coordinate x (panel (b)). As is easily seen, this function increases with an increasing driving force $\Delta/(\beta V)$ and time t . This is explained by the growth of the dendritic tip in the reference frame moving with the steady-state velocity V_{ss} . As can be easily understood, the velocity of this growth is constant and equal to V_{tr} .

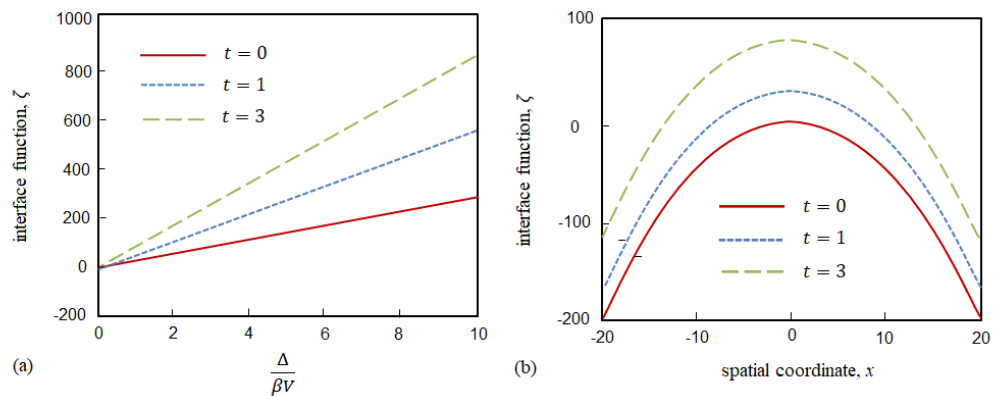


Figure 2. (a) The interface function ζ versus $\Delta/\beta V$ at fixed $x = 1$ and t . (b) The interface function ζ versus spatial coordinate x at fixed $\Delta/\beta V = 1$ and t . The calculations are made according to Equation (6).

3. Two-Dimensional BIE for Solidifying Pure and/or Binary Liquid

Let us now consider the case of crystal growth in a binary undercooled liquid with a solute concentration $C_{l\infty}$ in the binary liquid or solution far from the solid/liquid interface. In this case, the BIE takes the following form [9] (see also the Appendix A):

$$-\frac{Q}{mc_p} \left[\Delta - \frac{d_c}{\rho} K - \beta V_{ss} - \beta V_{ss} \frac{\partial \zeta}{\partial t} - I_\zeta^T \right] - C_{l\infty} = I_\zeta^C,$$

$$I_\zeta^C = \frac{(1 - k_0) P_C}{2\pi} \int_0^\infty \frac{d\tau}{\tau} \int_{-\infty}^\infty dx_1 C_i(x_1, t - \tau) \left(1 + \frac{\partial \zeta(x_1, t - \tau)}{\partial t} \right) \times \exp \left[-\frac{P_C}{2\tau} \left((x - x_1)^2 + (\zeta(x, t) - \zeta(x_1, t - \tau) + \tau)^2 \right) \right]. \tag{8}$$

Here, m and k_0 are the equilibrium liquid's slope and partition coefficient, respectively, $P_C = \rho V_{ss} / (2D_C)$, D_C is the diffusion coefficient, and C_i is the interfacial concentration.

Again, let us assume kinetically limited crystal growth with $K \approx -\partial^2 \zeta / \partial x^2$. This leads to $I_\zeta^T \rightarrow 0$ and $I_\zeta^C \rightarrow 0$. In this case, Equation (8) transforms to

$$\Delta + \frac{mc_p C_{l\infty}}{Q} + \frac{d_c}{\rho} \frac{\partial^2 \zeta}{\partial x^2} - \beta V_{ss} - \beta V_{ss} \frac{\partial \zeta}{\partial t} = 0. \tag{9}$$

Equation (9) can be solved using the Laplace transform by analogy with the aforementioned problem for a pure liquid. By omitting all mathematical manipulations, let us write out the final result as follows:

$$\zeta(x, t) = \left(\frac{\Delta Q + mc_p C_{l\infty}}{Q\beta V_{ss}} - 1 - \frac{d_c}{\beta V_{ss} \rho} \right) t - \frac{x^2}{2}. \tag{10}$$

This means that the translational velocity for a binary system becomes

$$V_{tr} = V_{ss} \left(\frac{\Delta Q + mc_p C_{l\infty}}{Q\beta V_{ss}} - 1 - \frac{d_c}{\beta V_{ss} \rho} \right). \tag{11}$$

As is easily seen, expression (11) transforms into expression (7) in the absence of a solute concentration, i.e., $C_{l\infty} = 0$.

4. Three-Dimensional BIE for a Paraboloid of Revolution and Elliptic Paraboloid Growing from Undercooled Binary Liquid

We now consider three-dimensional crystal growth in an undercooled binary melt or solution. Again, considering kinetically controlled interface motion (neglecting heat and mass transport), we write out the corresponding BIE in the form of

$$\Delta + \frac{mc_p C_{l\infty}}{Q} + \frac{d_c}{\rho} \left(\frac{\partial^2 \zeta}{\partial x^2} + \frac{\partial^2 \zeta}{\partial y^2} \right) - \beta V_{ss} - \beta V_{ss} \frac{\partial \zeta}{\partial t} = 0, \tag{12}$$

where the interface curvature is chosen as

$$K \approx -\frac{\partial^2 \zeta}{\partial x^2} - \frac{\partial^2 \zeta}{\partial y^2}$$

in the vicinity of a dendritic tip.

We solve this equation by analogy with the two-dimensional case. Considering the two shapes, a paraboloid of revolution and an elliptic paraboloid, we obtain the interface functions in the forms of

$$\zeta(x, y, t) = \left(\frac{\Delta Q + mc_p C_{l\infty}}{\beta V_{ss} Q} - \frac{2d_c}{\beta V_{ss} \rho} - 1 \right) t - \frac{x^2}{2} - \frac{y^2}{2}, \tag{13}$$

$$\zeta(x, y, t) = \left(\frac{\Delta Q + mc_p C_{l\infty}}{\beta V_{ss} Q} - \frac{2d_c}{\beta V_{ss} \rho (1 - a^2)} - 1 \right) t - \frac{x^2}{2(1 - a)} - \frac{y^2}{2(1 + a)}, \tag{14}$$

where a is the ellipticity parameter. The translation velocity for these two shapes has the respective forms of

$$V_{tr} = \begin{cases} V_{ss} \left(\frac{\Delta Q + mc_p C_{l\infty}}{\beta V_{ss} Q} - \frac{2d_c}{\beta V_{ss} \rho} - 1 \right), & \text{paraboloid of revolution,} \\ V_{ss} \left(\frac{\Delta Q + mc_p C_{l\infty}}{\beta V_{ss} Q} - \frac{2d_c}{\beta V_{ss} \rho (1 - a^2)} - 1 \right), & \text{elliptic paraboloid.} \end{cases} \tag{15}$$

Note that the second line of (15) transforms into the first line at $a = 0$ when an elliptical paraboloid becomes a paraboloid of revolution. In addition, the first line of (15) transforms into a two-dimensional case that accounts for the double curvature in three-dimensional geometry, i.e., $K_{3D} = 2K_{2D}$.

5. Conclusions

In summary, this paper addresses the BIE for the steady-state growth mode of dendritic crystals. First, we show that a dendrite whose tip is connected with the steady-state crystallization velocity V_{ss} grows in this reference frame with a constant translational velocity V_{tr} . As a result, the dendrite tip moves with a constant velocity $V = V_{ss} + V_{tr}$ in a laboratory reference frame. Accordingly, the same velocity V has been observed experimentally as the velocity of the recalescence front during the solidification of undercooled liquid droplets in electromagnetic levitators and other crystallization facilities (see, among others, [44,45]).

The constant translational crystallization velocity V_{tr} has been found to be a function of the established liquid undercooling Δ , dendrite tip diameter ρ , attachment kinetics of the atoms to the surface of the growing crystal β , steady-state velocity V_{ss} , and capillary constant d_c .

The main outcomes following from the aforementioned analysis are as follows:

(i) Considering kinetically limited crystal growth (neglecting heat and mass transport), we conclude that this process always occurs in a steady-state manner. In other words, there is no time to reach stationary growth, because the crystallization process is always in a steady state.

(ii) Moving to the frame of reference associated with the crystal surface (a system moving with the steady-state velocity V_{ss}), we see that a dendrite grows with a constant velocity V_{tr} in this system. Its growth is caused by the driving force (undercooling Δ) and the attachment of the atoms to the interphase boundary (kinetic parameter β). As this takes place, we can choose a reference frame that is always connected with the dendritic tip, i.e., $V_{tr} = 0$, if $V_{ss} = V = \Delta/\beta - d_c/(\beta\rho)$ for the two-dimensional solidification of a pure liquid (the reference frame following the growth of the crystal tip). In a more general case, we find this velocity from the second line of expression (15) as $V_{ss} = V = \Delta/\beta + mc_p C_{l\infty}/(\beta Q) - 2d_c/(\beta\rho(1 - a^2))$ for the three-dimensional thermodiffusion case.

(iii) Considering kinetically limited crystal growth (neglecting heat and mass transport), we can use the aforementioned expressions for $V_{ss} = V$ (at $V_{tr} = 0$) as auxiliary relations to find the selection constant entering the criterion of stable dendritic growth [10,20,46].

(iv) The translational velocity V_{tr} is defined by expressions (7), (11), or (15) in the case of kinetically limited crystallization when the integral contributions I_{ζ}^T and I_{ζ}^C are small enough. In a more general case, and especially in the case of rapid crystallization, V_{tr} should be numerically found from the BIE [10] that contains the integral contributions I_{ζ}^T and I_{ζ}^C .

(v) To move to a frame of reference moving together with the dendrite tip (moving with the constant velocity $V = V_{tr}$ relative to the laboratory coordinate system), we can choose $V_{ss} = 0$ (since this velocity is arbitrary). In this case, the BIE becomes

$$-\frac{Q}{mc_p} \left[\Delta - \frac{d_c}{\rho} K - \beta V \left(1 + \frac{\partial \zeta}{\partial t} \right) - I_{\zeta}^T \right] - C_{l\infty} = I_{\zeta}^C, \quad (16)$$

$$V = V_{tr} = \frac{\Delta Q + mc_p C_{l\infty}}{\beta Q} - \frac{2d_c}{\beta \rho (1 - a^2)},$$

where I_{ζ}^T and I_{ζ}^C are defined by expressions (1) and (8), respectively, with $P_T = \rho V / (2D_T)$ and $P_C = \rho V / (2D_C)$. Here, the characteristic spatial and time scales are chosen in terms of ρ and ρ/V , respectively. As this takes place, the Ivantsov solutions and selection criterion should be written in terms of V . Note that the second line of Equation (16) takes place only when $\beta \neq 0$.

The present theory can be extended to high-speed crystallization processes, which are described by a more complex BIE that takes into account the rate of atomic jumps to neighboring vacant positions [10]. From a mathematical point of view, such processes are described by the hyperbolic equation of impurity diffusion changing the concentration part of the BIE. In addition, the presence of a constant translational velocity V_{tr} (the growth velocity of the dendritic tip in any reference frame moving with the steady-state velocity V_{ss} with respect to the laboratory reference frame) should be taken into account when considering the evolution of various patterns and solid/liquid interfaces [37,47–54].

Author Contributions: Conceptualization, E.A.T. and D.V.A.; methodology, E.A.T. and D.V.A.; software, E.A.T., P.K.G., M.A.N., and L.V.T.; validation, E.A.T., P.K.G., M.A.N., and D.V.A.; formal analysis, E.A.T. and D.V.A.; investigation, E.A.T., P.K.G., M.A.N., L.V.T., and D.V.A.; resources, P.K.G. and D.V.A.; writing—original draft preparation, E.A.T., P.K.G., M.A.N., L.V.T., and D.V.A.; writing—review and editing, E.A.T., P.K.G., M.A.N., L.V.T., and D.V.A.; visualization, E.A.T., P.K.G., and L.V.T.; supervision, P.K.G. and D.V.A.; project administration, E.A.T. and D.V.A.; funding acquisition, E.A.T., P.K.G., M.A.N., L.V.T., and D.V.A. All authors have read and agreed to the published version of the manuscript.

Funding: M.A.N. acknowledges the research funding from the Ministry of Science and High Education of the Russian Federation (Ural Federal University Program of Development within the Priority-2030 Program).

Data Availability Statement: All data generated or analysed during this study are included in this published article.

Acknowledgments: We thank Dieter Herlach, Markus Rettenmayr, and Eugeny Makoveeva for their fruitful collaborations and discussions, as well as for providing research advice on dendritic growth, crystallization, and structure formation in undercooled liquids. The numerical calculations were performed using the supercomputer ‘URAN’ of IMM UB RAS, Ekaterinburg, Russia.

Conflicts of Interest: The authors declare no conflict of interest.

Appendix A

Let us now demonstrate how to derive the boundary integral Equations (1) and (8) analyzed above when considering pure thermal and thermochemical dendritic growth. At first, we consider the most simple case of the pure thermal boundary-value problem when the solid/liquid interface propagates into an undercooled liquid due to proper thermal gradients. Physically, the preferable direction in space is controlled by the anisotropy of the surface energy and atomic kinetics. To derive the boundary integral for the interface function, we apply the Green’s function method previously considered in Refs. [55,56].

So, we consider a propagation of the curved solid/liquid interface into a pure undercooled liquid. The initial position of a flat interface lies in the x -plane (which is perpendicular to the growth direction z ; see Figure A1). A curved solid/liquid phase interface then

moves along the z axis and is characterized by the function $z_{\text{interface}} = \zeta(\mathbf{x}, t)$, where t is the process time. At the solid/liquid interface, we have the following Gibbs–Thomson and heat balance equations:

$$T = T_f - \frac{d_c Q}{c_p} K - \tilde{\beta} \left(V_{ss} + \frac{\partial \zeta}{\partial t} \right), \tag{A1}$$

$$D_T (\nabla T_s - \nabla T_l) \cdot d\mathbf{s} = \frac{Q}{c_p} \left(V_{ss} + \frac{\partial \zeta}{\partial t} \right) d^2x. \tag{A2}$$

Here, T stands for the temperature, T_f is the freezing temperature of a flat phase interface, $\tilde{\beta}$ is the anisotropic kinetic coefficient, $d\mathbf{s}$ is the vector of the surface area directed towards the liquid phase, indices “ s ” and “ l ” denote the solid and liquid substances, respectively, and the solid/liquid interface curvature K in the 2D and 3D geometries is given by the following:

$$K(\zeta) = -\frac{\partial^2 \zeta / \partial x^2}{\left[1 + (\partial \zeta / \partial x)^2 \right]^{3/2}}, \quad K(\zeta) = -\nabla \cdot \left[\frac{\nabla \zeta}{\sqrt{1 + (\nabla \zeta)^2}} \right]. \tag{A3}$$

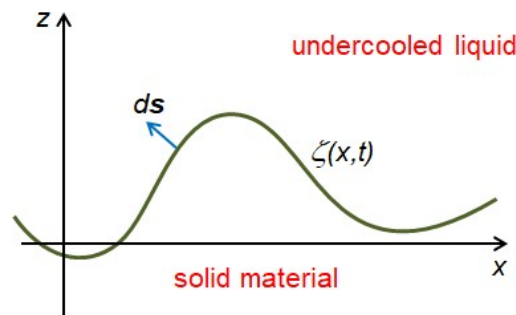


Figure A1. The solid/liquid interface $\zeta(x, t)$ moving into an undercooled liquid.

The temperature conductivity equation in the moving coordinate system reads as

$$\left(D_T \nabla^2 + V_{ss} \frac{\partial}{\partial z} - \frac{\partial}{\partial t} \right) T = 0. \tag{A4}$$

Using the Green’s function $G(p|p_1)$ for this equation, we have

$$\left(D_T \nabla_1^2 - V_{ss} \frac{\partial}{\partial z_1} + \frac{\partial}{\partial t_1} \right) G(p|p_1) = -\delta(p - p_1), \tag{A5}$$

where δ is the unit impulse, p denotes the point (\mathbf{x}, z, t) , and G equals zero at $t_1 > t$.

Next, we multiply the expressions (A4) and (A5) by G and T , subtract one equation from the other, and integrate the obtained formula. As a consequence, we obtain

$$\begin{aligned} T(p) = & D_T \int_{-\infty}^t dt_1 \int_{S_1} d\mathbf{s}_1 [T(p_1) \nabla_1 G(p|p_1) - G(p|p_1) \nabla_1 T(p_1)] \\ & + V_{ss} \int_{-\infty}^t dt_1 \int_{\Lambda_1} d^2x_1 dz_1 \frac{\partial}{\partial z_1} [G(p|p_1) T(p_1)]. \end{aligned} \tag{A6}$$

Here, Λ_1 is a domain including p and excluding the phase boundary, S_1 is the surface containing Λ_1 , and $d\mathbf{s}_1$ is the vector square on S_1 pointing along the normal to this surface.

Using the Fourier transform for the Green’s function from expression (A5), we obtain

$$G(p|p_1) = \int \frac{d^j k}{(2\pi)^j} \int_C \frac{d\omega}{2\pi} \hat{G}(\mathbf{k}, \omega) e^{i\mathbf{k}\cdot(\mathbf{r}-\mathbf{r}_1)+i\omega(t-t_1)}, \tag{A7}$$

where \mathbf{r} represents the vector (\mathbf{x}, z) , i stands for the imaginary unit, the path C passes from $-\infty$ to $+\infty$ and lies lower than all singularities in the ω plane to fulfill the causality condition [56], and the integral kernel looks like

$$\hat{G}(\mathbf{k}, \omega) = \frac{1}{D_T k^2 - iV_{ss}k_z + i\omega}. \tag{A8}$$

Let us especially underline that $j = 2$ and $j = 3$ in the 2D and 3D geometries, respectively.

By integrating expression (A7) and using the inverse Fourier transform on expression (A8), we come to

$$G(p|p_1) = \frac{1}{(4\pi D_T \tau)^{j/2}} \exp\left(-\frac{\Sigma^2}{4D_T \tau}\right),$$

$$\tau = t - t_1, \Sigma^2 = |\mathbf{x} - \mathbf{x}_1|^2 + (z - z_1 + V_{ss}\tau)^2. \tag{A9}$$

The condition of temperature continuity in the vicinity of the phase boundary leads to the conclusion that the summand proportional to $\nabla_1 G$ in (A6) vanishes. By evaluating the second integral summand with $\nabla_1 T$ in (A6) using expression (A2) and assuming that the last summand in (A6) gives T_∞ [56], we obtain

$$T(p) = T_\infty + \frac{Q}{c_p} \int_{-\infty}^t dt_1 \int_{-\infty}^{\infty} \int_{-\infty}^{\infty} d^2 x_1 G(p|p_1) \left(V_{ss} + \frac{\partial \zeta_1}{\partial t_1} \right). \tag{A10}$$

Here, T_∞ represents the far-field temperature, and ζ_1 means $\zeta(\mathbf{x}_1, t_1)$.

Now, we bring the point p closer to the phase boundary and combine expressions (A1) and (A10):

$$\Delta - d_c K - \beta \left(V_{ss} + \frac{\partial \zeta}{\partial t} \right) - \int_{-\infty}^t dt_1 \int_{-\infty}^{\infty} \int_{-\infty}^{\infty} d^2 x_1 \bar{G}(p|p_1) \left(V_{ss} + \frac{\partial \zeta(\mathbf{x}_1, t_1)}{\partial t_1} \right) = 0. \tag{A11}$$

Here, $\Delta = (T_f - T_\infty)c_p/Q$ stands for the dimensionless melt undercooling, $\beta = \tilde{\beta}c_p/Q$ stands for the kinetic coefficient,

$$\bar{G}(p|p_1) = \frac{1}{(4\pi D_T \tau)^{j/2}} \exp\left(-\frac{\bar{\Sigma}^2}{4D_T \tau}\right),$$

$$\bar{\Sigma}^2 = |\mathbf{x} - \mathbf{x}_1|^2 + [\zeta(\mathbf{x}, t) - \zeta(\mathbf{x}_1, t_1) + V_{ss}\tau]^2.$$

Now, we introduce the dimensionless variables as follows (ρ means a typical length):

$$x' = \frac{x}{\rho}, x'_1 = \frac{x_1}{\rho}, \tau' = \frac{V_{ss}\tau}{\rho}, \zeta' = \frac{\zeta}{\rho}, t' = \frac{V_{ss}t}{\rho}, t'_1 = \frac{V_{ss}t_1}{\rho}, \tau' = t' - t'_1.$$

Expression (A11) becomes (for simplicity, we omitted all primes):

$$\Delta - \frac{d_c}{\rho} K - \beta V_{ss} \left(1 + \frac{\partial \zeta(\mathbf{x}, t)}{\partial t} \right) = I_\zeta^T. \tag{A12}$$

Here, the right-hand side reads as

$$I_{\zeta}^T = P_T \int_0^{\infty} \frac{d\tau}{2\pi\tau} \int_{-\infty}^{\infty} dx_1 \left[1 + \frac{\partial\zeta(x_1, t - \tau)}{\partial t} \right] \times \exp \left\{ -\frac{P_T}{2\tau} \left[(x - x_1)^2 + (\zeta(x, t) - \zeta(x_1, t - \tau) + \tau)^2 \right] \right\} \tag{A13}$$

in the 2D geometry, and as

$$I_{\zeta}^T = P_T^{3/2} \int_0^{\infty} \frac{d\tau}{(2\pi\tau)^{3/2}} \int_{-\infty}^{\infty} \int_{-\infty}^{\infty} d^2x_1 \left[1 + \frac{\partial\zeta(\mathbf{x}_1, t - \tau)}{\partial t} \right] \times \exp \left\{ -\frac{P_T}{2\tau} \left[|\mathbf{x} - \mathbf{x}_1|^2 + (\zeta(\mathbf{x}, t) - \zeta(\mathbf{x}_1, t - \tau) + \tau)^2 \right] \right\} \tag{A14}$$

in the 3D geometry. Here, $P_T = \rho V_{ss}/(2D_T)$ stands for the thermal Péclet number, and $K(\zeta(x, t))$ is defined by the formulas in (A3). Let us especially highlight that Equation (A12) is the rescaled law for the phase boundary migration during the crystallization of a single-component undercooled melt. This equation describes both the 2D and 3D cases of the interface motion.

As a special note, expressions (A12) and (A13) in the two-dimensional geometry match the previous studies of morphological stability and growth mode selection for dendritic crystals [19–22,35]. In the three-dimensional geometry, assuming that $\partial\zeta/\partial t = 0$ and $\tilde{\beta} = 0$, we conclude that Equations (A12) and (A14) match the equations from previous works [17,47]. Also, note that Equations (A12)–(A14) were studied in [18] in the case of $\tilde{\beta} = 0$ when dealing with the two- and three-dimensional geometries of crystal growth.

Let us now consider the phase interface motion controlled by the simultaneous occurrence of thermal and concentration gradients. As this takes place, the anisotropy of the crystal surface energy and the atomic kinetics define the preferable direction of the interface motion. The process under question takes place in undercooled binary melts and solutions when the diffusion of dissolved impurities plays an important role in the dynamics of a curved solid/liquid phase boundary.

We consider an undercooled binary liquid consisting of noninteracting particles of two types: particles of type A (e.g., the solvent) and particles of type B (e.g., the dissolved substance). In addition, we assume that isobaric conditions take place in the non-isothermal liquid being considered, under which crystallization occurs without a change in the mass density, i.e., we neglect shrinkage when the substance passes from the liquid state to the solid form. We also assume that the heat and mass transfer in the liquid and at the interfacial boundary occur according to the conductive mechanism. In other words, we consider that there is no convection in the liquid. Moreover, we shall be neglectful of the chemical diffusion in the solid material owing to its much slower rate as compared to the diffusion in the liquid (see the typical estimates in [57–59]). These hypotheses enable us to write down the mass balance equation at the moving phase boundary in the form of

$$-D_C \nabla C_l \cdot ds = (1 - k_0) C_i \left(V + \frac{\partial\zeta}{\partial t} \right) d^2x, \tag{A15}$$

where C_l stands for the solute concentration of a dissolved component, and C_i is the solute concentration at the curved solid/liquid boundary. The phase transition temperature at this boundary when considering a binary system reads as

$$T = T_f - \frac{d_c Q}{c_p} K + m C_i - \tilde{\beta} \left(V_{ss} + \frac{\partial\zeta}{\partial t} \right). \tag{A16}$$

The transport of dissolved impurities in the moving coordinate system is given by a diffusion equation:

$$\left(D_C \nabla^2 + V_{ss} \frac{\partial}{\partial z} - \frac{\partial}{\partial t} \right) C_l = 0. \tag{A17}$$

It should be mentioned that the implementation of atomic kinetics into thermal and thermosolutal models of the phase interface motion, expressions (A1) and (A16), has been made earlier using alternative approaches [60,61]. This allows us to provide a sufficiently transparent description of the thermochemical phenomena for different steps of patterns evolution.

Taking the consistency of Equations (A4) and (A17) into account, we can change D_T to D_C and derive by analogy with Equation (A6) the solute concentration:

$$C_l(p) = D_C \int_{-\infty}^t dt_1 \int_{S_1} d\mathbf{s}_1 \{ \nabla_1 [C_l(p_1) G_C(p|p_1)] - 2G_C(p|p_1) \nabla_1 C_l(p_1) \} + V_{ss} \int_{-\infty}^t dt_1 \int_{\Lambda_1} d^2x_1 dz_1 \frac{\partial}{\partial z_1} [G_C(p|p_1) C_l(p_1)]. \tag{A18}$$

Note that the integral of the contribution $\nabla_1 [C_l(p_1) G_C(p|p_1)]$ vanishes on the basis of the Kelvin–Stokes theorem (when integrating the ∇ operator about a closed loop S_1).

The integral of the contribution with $G_C(p|p_1) \nabla_1 C_l(p_1)$ can be calculated using expression (A15) when the concentration flux into the solid material is infinitely small. The last contribution is equivalent to the far-field solute concentration $C_{l\infty}$ in the melt (see, for details, [56]). Keeping this in mind, we rewrite (A18) in the form of

$$C_l(p) = C_{l\infty} + 2(1 - k_0) \int_{-\infty}^t dt_1 \int_{-\infty}^{\infty} \int_{-\infty}^{\infty} d^2x_1 G_C(p|p_1) C_i(\mathbf{x}_1, t_1) \left(V_{ss} + \frac{\partial \zeta_1}{\partial t_1} \right), \tag{A19}$$

$$G_C(p|p_1) = \frac{1}{2(4\pi D_C \tau)^{j/2}} \exp\left(-\frac{\Sigma^2}{4D_C \tau}\right).$$

By combining Equations (A12) and (A16), we derive the interfacial concentration as follows

$$C_i(\mathbf{x}, t) = -\frac{Q}{mc_p} \left[\Delta - \frac{d_c}{\rho} K - \beta V_{ss} \left(1 + \frac{\partial \zeta(\mathbf{x}, t)}{\partial t} \right) - I_{\zeta}^T \right]. \tag{A20}$$

Now, Equations (A19) and (A20) enable us to get the boundary integral equation for thermosolutal model in the form of

$$-\frac{Q}{mc_p} \left[\Delta - \frac{d_c}{\rho} K - \beta V_{ss} \left(1 + \frac{\partial \zeta(\mathbf{x}, t)}{\partial t} \right) - I_{\zeta}^T \right] - C_{l\infty} = I_{\zeta}^C \tag{A21}$$

with

$$I_{\zeta}^C = (1 - k_0) P_C \int_0^{\infty} \frac{d\tau}{2\pi\tau} \int_{-\infty}^{\infty} dx_1 C_i(x_1, t - \tau) \left[1 + \frac{\partial \zeta(x_1, t - \tau)}{\partial t} \right] \times \exp\left\{ -\frac{P_C}{2\tau} \left[(x - x_1)^2 + (\zeta(x, t) - \zeta(x_1, t - \tau) + \tau)^2 \right] \right\} \tag{A22}$$

in the 2D geometry and

$$I_{\zeta}^C = (1 - k_0) P_C^{3/2} \int_0^{\infty} \frac{d\tau}{(2\pi\tau)^{3/2}} \int_{-\infty}^{\infty} \int_{-\infty}^{\infty} d^2x_1 C_i(\mathbf{x}_1, t - \tau) \left[1 + \frac{\partial \zeta(x_1, t - \tau)}{\partial t} \right] \times \exp\left\{ -\frac{P_C}{2\tau} \left[|\mathbf{x} - \mathbf{x}_1|^2 + (\zeta(\mathbf{x}, t) - \zeta(\mathbf{x}_1, t - \tau) + \tau)^2 \right] \right\} \tag{A23}$$

in the 3D geometry. Here, $P_C = \rho V_{ss}/(2D_C) = P_T D_T/D_C$ is the solute concentration Péclet number.

In summary, the derived integrals (A13) and (A14) for the pure thermal problem and (A22) and (A23) for the concentration problem define the general thermosolutal boundary integral Equation (A21). This equation defines the interface function $\zeta(\mathbf{x}, t)$ defining the propagation of the curved crystallization front into an undercooled binary liquid.

This equation contains the case of the pure chemical problem, which follows from (A21) using the limiting transitions $D_T \rightarrow \infty$ and $P_T \rightarrow 0$ when I_C^T , defined by expressions (A13) and (A14), becomes negligibly small.

Let us especially highlight that the boundary integral Equation (A21) with the integral contributions (A13), (A14), (A22), and (A23) should be solved analytically and/or numerically for various shapes of growing patterns and different crystallization conditions (e.g., for steady and unsteady crystal growth scenarios). For example, the evolution of dendrite tips, envelops, and primary stems, as well as the dendrite tip velocity and tip diameter, can be found using this equation. When dealing with the unsteady growth of various patterns and structures, we can answer the question about their nonstationary time evolution and their approaching steady-state conditions on the basis of the single integral differential Equation (A21). The answer to this question is significant when it comes to describing the materials microstructures obtained in certain crystallization conditions.

References

- Mullin, J.W. *Crystallization*; Butterworths: London, UK, 1972.
- Borisov, V.T. *Theory of Two-Phase Zone of a Metal Ingot*; Metallurgiya Publishing House: Moscow, Russia, 1987.
- Slezov, V.V. *Kinetics of First-Order Phase Transitions*; Wiley-VCH: Weinheim, Germany, 2009.
- Kurz, W.; Fisher, D.J.; Trivedi, R. Progress in modelling solidification microstructures in metals and alloys: Dendrites and cells from 1700 to 2000. *Int. Mater. Rev.* **2019**, *64*, 311–354. [[CrossRef](#)]
- Makoveeva, E.V. Steady-state crystallization with a mushy layer: A test of theory with experiments. *Eur. Phys. J. Spec. Top.* **2023**, *232*, 1165–1169. [[CrossRef](#)]
- Makoveeva, E.V.; Alexandrov, D.V.; Galenko, P.K. The impact of convection on morphological instability of a planar crystallization front. *Int. J. Heat Mass Trans.* **2023**, *217*, 124654. [[CrossRef](#)]
- Nash, G.E. *Capillary-Limited, Steady State Dendritic Growth. Part I. Theoretical Development*; NRL Report; Publisher: Naval Research Laboratory, USA, May 1974.
- Nash, G.E.; Glicksman, M.E. Capillary-limited steady-state dendritic growth—I. Theoretical development. *Acta Metall.* **1974**, *22*, 1283–1290. [[CrossRef](#)]
- Alexandrov, D.V.; Galenko, P.K. Boundary integral approach for propagating interfaces in a binary non-isothermal mixture. *Phys. A* **2017**, *469*, 420–428. [[CrossRef](#)]
- Alexandrov, D.V.; Galenko, P.K. Selection criterion of stable mode of dendritic growth with n-fold symmetry at arbitrary Péclet numbers with a forced convection. In *IUTAM Symposium on Recent Advances in Moving Boundary Problems in Mechanics, Proceedings of the IUTAM Symposium on Moving Boundary Problems, Christchurch, New Zealand, 12–15 February 2018*; Springer: Cham, Switzerland, 2019; pp. 203–215.
- Saville, D.A.; Beaghton, P.J. Growth of needle-shaped crystals in the presence of convection. *Phys. Rev. A* **1988**, *37*, 3423–3430. [[CrossRef](#)]
- Titova, E.A.; Alexandrov, D.V. The boundary integral equation for curved solid/liquid interfaces propagating into a binary liquid with convection. *J. Phys. A Math. Theor.* **2022**, *55*, 055701. [[CrossRef](#)]
- Alexandrov, D.V.; Toropova, L.V. The role of incoming flow on crystallization of undercooled liquids with a two-phase layer. *Sci. Rep.* **2022**, *12*, 17857. [[CrossRef](#)]
- Pelce, P.; Pomeau, Y. Dendrites in the small undercooling limit. *J. Stud. Appl. Math.* **1986**, *74*, 245–258. [[CrossRef](#)]
- Ben Amar, M.; Pomeau, Y. Theory of dendritic growth in a weakly undercooled melt. *Europhys. Lett.* **1986**, *2*, 307–314. [[CrossRef](#)]
- Ben Amar, M. Theory of needle-crystal. *Phys. D* **1988**, *31*, 409–423. [[CrossRef](#)]
- Barbieri, A.; Hong, D.C.; Langer, J.S. Velocity selection in the symmetric model of dendritic crystal growth. *Phys. Rev. A* **1987**, *35*, 1802–1808. [[CrossRef](#)]
- Barbieri, A.; Langer, J.S. Predictions of dendritic growth rates in the linearized solvability theory. *Phys. Rev. A* **1989**, *39*, 5314–5325. [[CrossRef](#)] [[PubMed](#)]
- Barber, M.N.; Barbieri, A.; Langer, J.S. Dynamics of dendritic sidebranching in the two-dimensional symmetric model of solidification. *Phys. Rev. A* **1987**, *36*, 3340–3349. [[CrossRef](#)] [[PubMed](#)]
- Brener, E.A.; Mel'nikov, V.A. Pattern selection in two-dimensional dendritic growth. *Adv. Phys.* **1991**, *40*, 53–97. [[CrossRef](#)]

21. Barbieri, A. Velocity selection at large undercooling in a two-dimensional nonlocal model of solidification. *Phys. Rev. A* **1987**, *36*, 5353–5358. [[CrossRef](#)]
22. Brener, E.A.; Mel'nikov, V.A. Two-dimensional dendritic growth at arbitrary Peclet number. *J. Phys. Fr.* **1990**, *51*, 157–166. [[CrossRef](#)]
23. Galenko, P.K.; Alexandrov, D.V.; Titova, E.A. The boundary integral theory for slow and rapid curved solid/liquid interfaces propagating into binary systems. *Philos. Trans. R. Soc. A* **2018**, *376*, 20170218. [[CrossRef](#)]
24. Tong, X.; Beckermann, C.; Karma, A.; Li, Q. Phase-field simulations of dendritic crystal growth in a forced flow. *Phys. Rev. E* **2001**, *63*, 061601. [[CrossRef](#)]
25. Jeong, J.-H.; Goldenfeld, N.; Dantzig, J.A. Phase field model for three-dimensional dendritic growth with fluid flow. *Phys. Rev. E* **2001**, *64*, 041602. [[CrossRef](#)]
26. Toropova, L.V.; Galenko, P.K.; Alexandrov, D.V.; Rettenmayr, M.; Kao, A.; Demange, G. Non-axisymmetric growth of dendrite with arbitrary symmetry in two and three dimensions: Sharp interface model vs phase-field model. *Eur. Phys. J. Spec. Top.* **2020**, *229*, 2899–2909. [[CrossRef](#)]
27. Makoveeva, E.V. Mathematical modeling of the crystal growth process in a binary system. *AIP Conf. Proc.* **2020**, *2313*, 030058.
28. Makoveeva, E.V. The effect of nonlinear growth rates of crystals on the evolution of particulate ensembles in binary liquids. *AIP Conf. Proc.* **2020**, *2259*, 020005.
29. Zhu, C.-S.; Li, T.-Y.; Zhao, B.-R.; Wang, C.-L.; Gao, Z.-H. Simulation of inclined dendrites under natural convection by KKS phase field model based on CUDA. *China Foundry* **2023**, *20*, 432–442. [[CrossRef](#)]
30. Teraoka, Y.; Saito, A.; Okawa, S. Ice crystal growth in supercooled solution. *Int. J. Refrig.* **2002**, *25*, 218–225. [[CrossRef](#)]
31. Demange, G.; Zapolsky, H.; Patte, R.; Brunel, M. Growth kinetics and morphology of snowflakes in supersaturated atmosphere using a three-dimensional phase-field model. *Phys. Rev. E* **2017**, *96*, 022803. [[CrossRef](#)]
32. Makoveeva, E.V. An exact analytical solution to the nonstationary coagulation equation describing the endosomal network dynamics. *Math. Meth. Appl. Sci.* **2022**. [[CrossRef](#)]
33. Titova, E.A.; Galenko, P.K.; Alexandrov, D.V. Method of evaluation for the non-stationary period of primary dendritic crystallization. *J. Phys. Chem. Solids* **2019**, *134*, 176–181. [[CrossRef](#)]
34. Chan, S.K.; Reimer, H.H.; Kahlweit, M. On the stationary growth shapes of NH₄Cl dendrites. *J. Cryst. Growth* **1976**, *326*, 303–315. [[CrossRef](#)]
35. Brener, E.A. Effects of surface energy and kinetics on the growth of needle-like dendrites. *J. Cryst. Growth* **1990**, *99*, 165–170. [[CrossRef](#)]
36. Makoveeva, E.V. Mathematical modeling of nonlinear growth rates of crystals with allowance for Meirs kinetics. *AIP Conf. Proc.* **2019**, *2174*, 020136.
37. Alexandrov, D.V.; Galenko, P.K. The shape of dendritic tips. *Philos. Trans. R. Soc. A* **2020**, *378*, 20190243. [[CrossRef](#)] [[PubMed](#)]
38. Hoyt, J.J.; Sadigh, B.; Asta, M.; Foiles, S.M. Kinetic phase field parameters for the Cu-Ni system derived from atomistic computations. *Acta Mater.* **1999**, *47*, 3181–3187. [[CrossRef](#)]
39. Mendeleev, M.I.; Rahman, M.J.; Hoyt, J.J.; Asta, M. Molecular-dynamics study of solid-liquid interface migration in fcc metals. *Model. Simul. Mater. Sci. Eng.* **2010**, *18*, 074002. [[CrossRef](#)]
40. Makoveeva, E.V.; Ivanov, A.A. Analysis of an integro-differential model for bulk continuous crystallization with account of impurity feeding, dissolution/growth of nuclei and removal of product crystals. *Math. Meth. Appl. Sci.* **2023**. [[CrossRef](#)]
41. Xie, Y.; Dong, H.; Dantzig, J. Growth of secondary dendrite arms of Fe-C alloy during transient directional solidification by phase-field method. *ISI J. Int.* **2014**, *54*, 430–436. [[CrossRef](#)]
42. Ditkin, V.A.; Prudnikov, A.P. *Integral Transforms and Operational Calculus*; Pergamon Press: Oxford, UK, 1965.
43. von Doetsch, G. *Anleitung zum Praktischen Gebrauch der Laplace-Transformation und der Z-Transformation*; R. Oldenbourg: München, Germany, 1961.
44. Reinartz, M.; Kolbe, M.; Herlach, D.M.; Rettenmayr, M.; Toropova, L.V.; Alexandrov, D.V.; Galenko, P.K. Study on anomalous rapid solidification of Al-35 at%Ni in microgravity. *JOM* **2022**, *74*, 2420–2427. [[CrossRef](#)]
45. Galenko, P.K.; Toropova, L.V.; Alexandrov, D.V.; Phanikumar, G.; Assadi, H.; Reinartz, M.; Paul, P.; Fang, Y.; Lippmann, S. Anomalous kinetics, patterns formation in recalescence, and final microstructure of rapidly solidified Al-rich Al-Ni alloys. *Acta Mater.* **2022**, *241*, 118384. [[CrossRef](#)]
46. Alexandrov, D.V.; Galenko, P.K. A review on the theory of stable dendritic growth. *Philos. Trans. R. Soc. A* **2021**, *379*, 20200325. [[CrossRef](#)] [[PubMed](#)]
47. Pélce, P. *Dynamics of Curved Fronts*; Academic Press: Boston, MA, USA, 1988.
48. Nizovtseva, I.G.; Ivanov, A.A.; Alexandrova, I.V. Approximate analytical solution of the integro-differential model of bulk crystallization in a metastable liquid with mass supply (heat dissipation) and crystal withdrawal mechanism. *Math. Meth. Appl. Sci.* **2022**, *45*, 8170–8178. [[CrossRef](#)]
49. Libbrecht, K. *Snowflakes*; Voyageur Press: Minneapolis, MN, USA, 2004.
50. Libbrecht, K.G. The formation of snow crystals. *Am. Sci.* **2007**, *95*, 52–59. [[CrossRef](#)]
51. Makoveeva, E.V. Mathematical modeling of nonlinear crystal growth rates in binary systems. *AIP Conf. Proc.* **2020**, *2216*, 030004.
52. Makoveeva, E.V.; Tsvetkov, I.N.; Ryashko, L.B. Stochastically-induced dynamics of earthquakes. *Eur. Math. Meth. Appl. Sci.* **2022**. [[CrossRef](#)]

53. Makoveeva, E.V.; Alexandrov, D.V.; Ivanov, A.A.; Alexandrova, I.V. Desupersaturation dynamics in solutions with applications to bovine and porcine insulin crystallization. *J. Phys. A: Math. Theor.* **2023**, *56*, 455702. [[CrossRef](#)]
54. Almgren, R.; Dai, W.-S.; Hakim, V. Scaling behavior in anisotropic Hele-Shaw flow. *Phys. Rev. Lett.* **1993**, *71*, 3461–3464. [[CrossRef](#)]
55. Langer, J.S.; Turski, L.A. Studies in the theory of interfacial stability—I. Stationary symmetric model. *Acta Metall.* **1977**, *25*, 1113–1119. [[CrossRef](#)]
56. Langer, J.S. Studies in the theory of interfacial stability—II. Moving symmetric model. *Acta Metall.* **1977**, *25*, 1121–1137. [[CrossRef](#)]
57. Flemings, M.C. *Solidification Processing*; McGraw-Hill: New York, NY, USA, 1974.
58. Lyubov, B.Y. *Theory of Crystallization in Large Volumes*; Nauka: Moscow, Russia, 1975.
59. Gupta, S.C. *Classical Stefan Problem*; Elsevier: Amsterdam, The Netherlands, 2003.
60. Ben Amar, M. Dendritic growth rate at arbitrary undercooling. *Phys. Rev. A* **1990**, *41*, 2080–2092. [[CrossRef](#)]
61. Conti, M. Thermal and chemical diffusion in the rapid solidification of binary alloys. *Phys. Rev. E* **2000**, *61*, 642–650. [[CrossRef](#)]

Disclaimer/Publisher’s Note: The statements, opinions and data contained in all publications are solely those of the individual author(s) and contributor(s) and not of MDPI and/or the editor(s). MDPI and/or the editor(s) disclaim responsibility for any injury to people or property resulting from any ideas, methods, instructions or products referred to in the content.